Fast and Radiation Hard Inorganic Scintillators for Future HEP Experiments

Chen Hu, Liyuan Zhang, and Ren-Yuan Zhu

HEP Crystal Laboratory, California Institute of Technology, Pasadena, CA 91125, USA

1. Introduction

Future HEP experiments at the energy and intensity frontiers require fast and ultrafast inorganic scintillators with excellent radiation hardness to face the challenges of unprecedented event rate and severe radiation environment. We report recent progress in fast and ultrafast inorganic scintillators for future HEP experiments. Examples are LYSO crystals and LuAG ceramics for an ultra-compact shashlik sampling calorimeter for the HL-LHC and the proposed FCC-hh, and yttrium doped BaF_2 crystals for the proposed Mu2e-II experiment. Applications for Gigahertz hard X-ray imaging will also be discussed.

Table I shows scintillation performance of fast and ultrafast inorganic scintillators. LYSO crystals and LuAG:Ce ceramics show high stopping power, high light output, short decay time and good radiation hardness against ionization dose and hadrons. Yttrium doped BaF_2 crystal shows ultrafast scintillation light with sub-ns decay time and a suppressed slow scintillation light. These inorganic scintillators are promising for future HEP experiments.

Table I Scintillation Performance of Fast and Ultrafast Inorganic Scintillators

	BaF_2	BaF_2:Y	ZnO:Ga	YAP:Yb	YAG:Yb	β-Ga_2O_3	LYSO:Ce	LuAG:Ce	YAP:Ce	GAGG:Ce	LuYAP:Ce	YSO:Ce
Density (g/cm^3)	4.89	4.89	5.67	5.35	4.56	5.94[1]	7.4	6.76	5.35	6.5	7.2[f]	4.44
Melting points (°C)	1280	1280	1975	1870	1940	1725	2050	2060	1870	1850	1930	2070
X_0 (cm)	2.03	2.03	2.51	2.77	3.53	2.51	1.14	1.45	2.77	1.63	1.37	3.10
R_M (cm)	3.1	3.1	2.28	2.4	2.76	2.20	2.07	2.15	2.4	2.20	2.01	2.93
λ_I (cm)	30.7	30.7	22.2	22.4	25.2	20.9	20.9	20.6	22.4	21.5	19.5	27.8
Z_{eff}	51.6	51.6	27.7	31.9	30	28.1	64.8	60.3	31.9	51.8	58.6	33.3
dE/dX (MeV/cm)	6.52	6.52	8.42	8.05	7.01	8.82	9.55	9.22	8.05	8.96	9.82	6.57
λ_{peak} [a] (nm)	300 220	300 220	380	350	350	380	420	520	370	540	385	420
Refractive Index[b]	1.50	1.50	2.1	1.96	1.87	1.97	1.82	1.84	1.96	1.92	1.94	1.78
Normalized Light Yield[a,c]	42 4.8	1.7 4.8	6.6[d]	0.19[d]	0.36[d]	6.5 0.5	100	35[e] 48[e]	9 32	115	16 15	80
Total Light yield (ph/MeV)	13,000	2,000	2,000[d]	57[d]	110[d]	2,100	30,000	25,000[e]	12,000	34,400	10,000	24,000
Decay time[a] (ns)	600 0.5	600 0.5	<1	1.5	4	148 6	40	820 50	191 25	53	1485 36	75
LY in 1st ns (photons/MeV)	1200	1200	610[d]	28[d]	24[d]	43	740	240	391	640	125	318
40 keV Att. Leng. (1/e, mm)	0.106	0.106	0.407	0.314	0.439	0.394	0.185	0.251	0.314	0.319	0.214	0.334

2. Bright, Fast and Radiation Hard LYSO:Ce and LuAG:Ce

2.1 LYSO:Ce Crystals and LuAG:Ce Ceramics

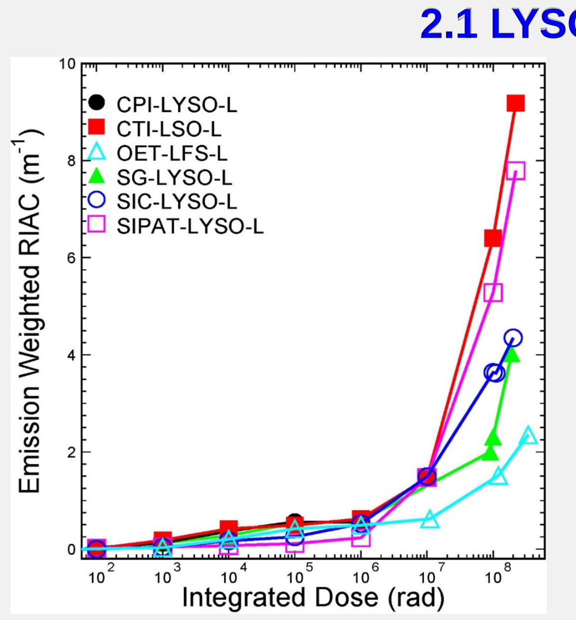

Fig. 1 Emission weighted RIAC values as a function of integrated dose for 20 cm long LYSO crystals from various vendors.

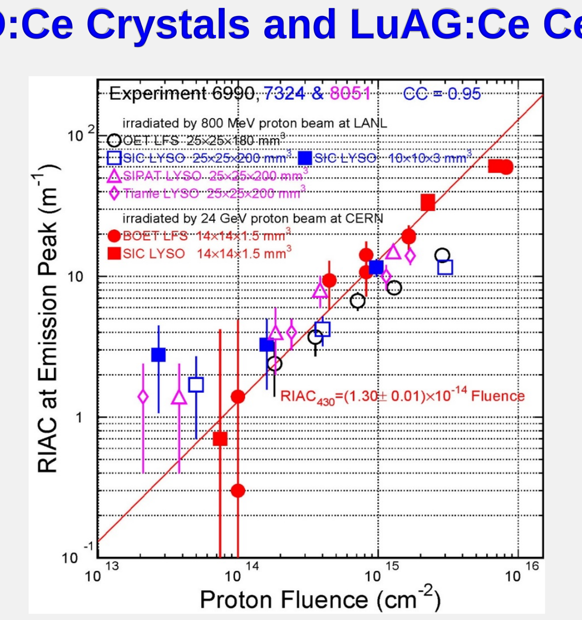

Fig. 2 The RIAC values as a function of proton fluence for LYSO crystals from various vendors.

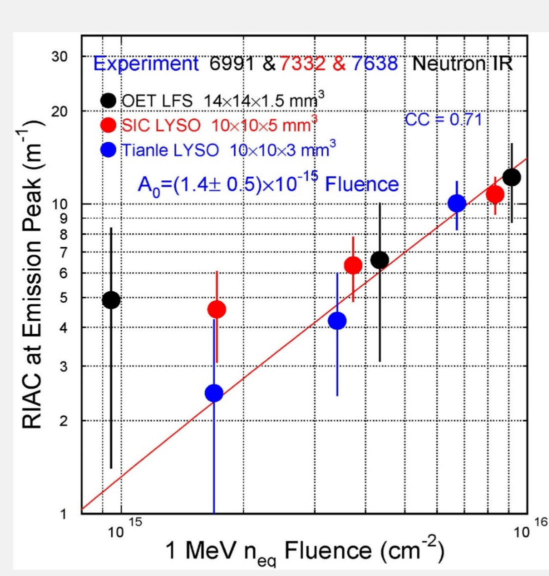

Fig. 3 The RIAC values as a function of 1 MeV equivalent neutron fluence for LYSO crystals from various vendors.

Figs. 1, 2, and 3 show respectively the radiation induced absorption coefficient (RIAC) values as a function of (1) integrated dose, (2) proton fluence, and (3) 1 MeV equivalent neutron fluence for LYSO crystals from various vendors. We found that damage induced by protons is an order of magnitude larger than that from neutrons due to ionization energy loss in addition to displacement and nuclear breakup. These results prove that LYSO crystals from different vendors satisfy CMS BTL specification: RIAC < 3 /m after 4.8 Mrad, 2.5×10^{13} p/cm² and 3×10^{14} n_{eq}/cm^2.

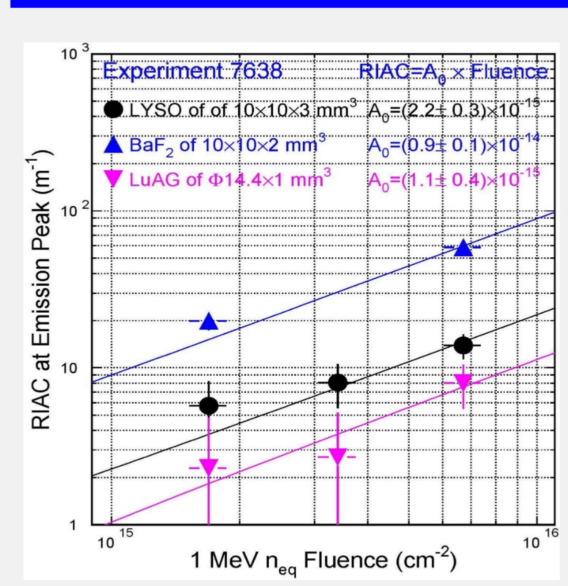

Fig. 4 The RIAC values as a function of 1 MeV equivalent neutron fluence for LYSO and BaF_2 crystals and LuAG:Ce ceramics.

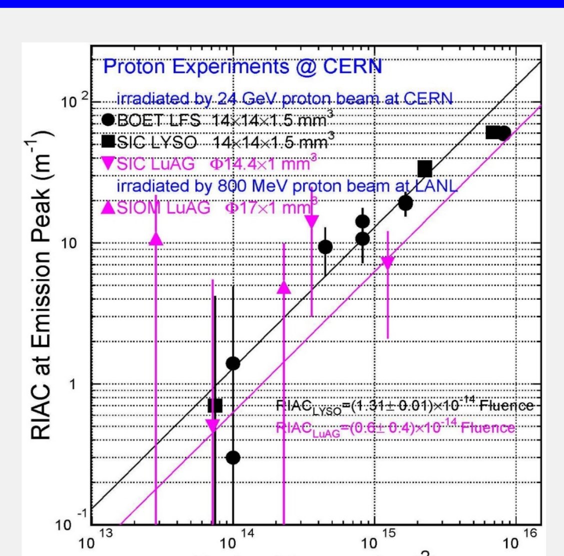

Fig. 5 The RIAC values as a function of proton fluence for LYSO crystals and LuAG:Ce ceramics.

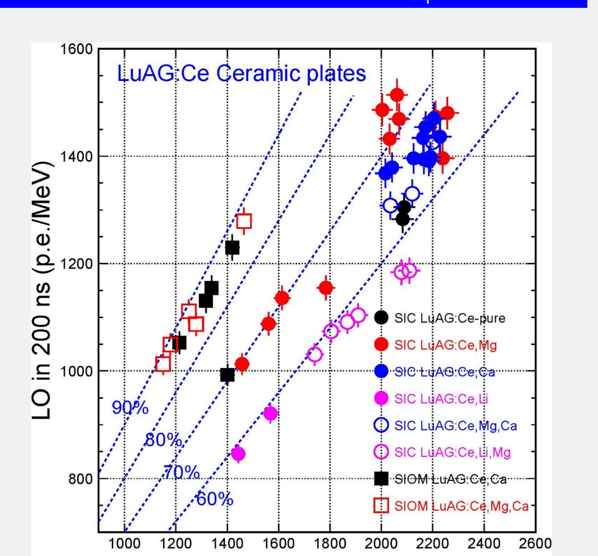

Fig. 6 Light output (LO) measured in 200 and 3,000 ns gates for LuAG:Ce ceramic samples with various co-dopings.

Figs. 4 and 5 show the RIAC values as a function of (1) 1 MeV equivalent neutron fluence and (2) proton fluence for LuAG:Ce ceramics and LYSO crystals. We found that LuAG:Ce ceramics show a factor of two better radiation hardness than LYSO crystals up to 6.7×10^{15} n_{eq}/cm^2 and 1.2×10^{15} p/cm², so are promising for the FCC-hh. Fig. 6 shows that Ca^{2+} co-doping suppresses improves the Fast/Total (F/T) ratio to 90%.

2.2 γ-Ray and Neutron Induced Readout Noise in LYSO+SiPM Packages

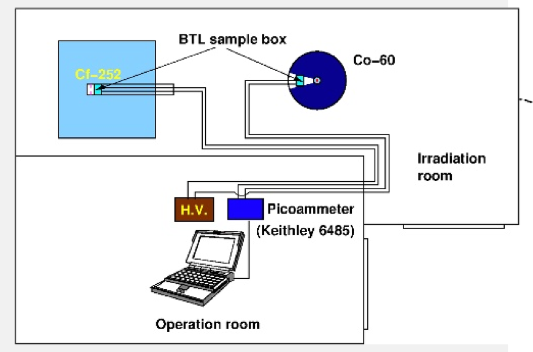

Fig. 7 The setup used to measure the radiation induced photocurrent and readout noise (RIN) in LYSO+SiPM before, during and after irradiation.

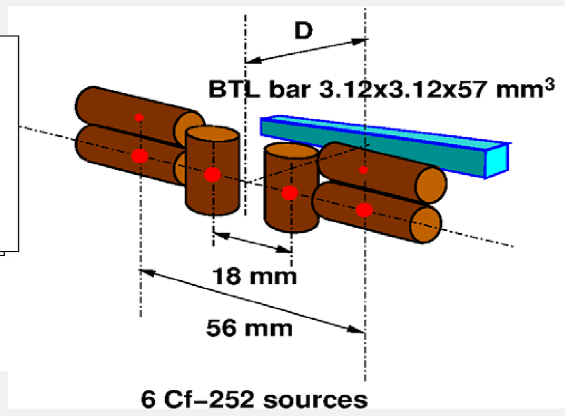

Fig. 8 Three Cf-252 source pairs used as the neutron source to measure the neutron induced photocurrent and readout noise in LYSO+SiPM packages.

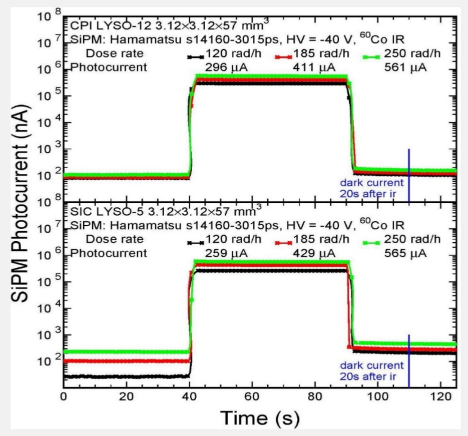

Fig. 9 Histories of the SiPM photocurrent for CPI-12 (top) and SIC-5 (bottom) LYSO bars with Co-60 γ-ray irradiation.

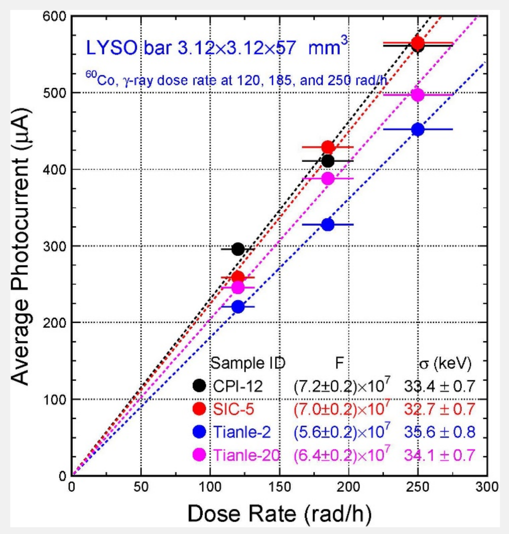

Fig. 10 Photocurrent is shown as a function of the dose rate for four LYSO+SiPM packages.

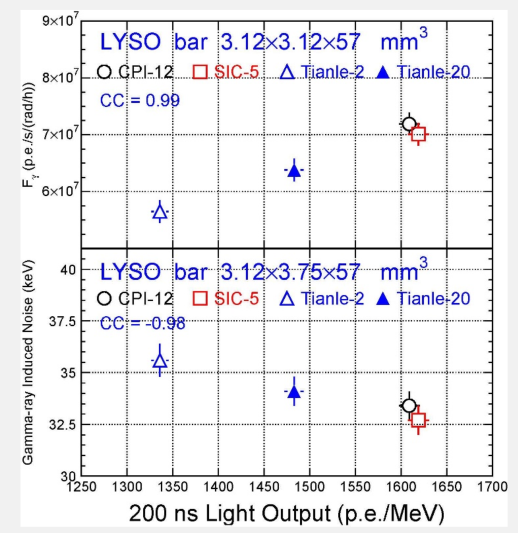

Fig. 11 Correlation between Fγ (top) and RIN:γ (bottom) vs. the LO in 200 ns for four LYSO+SiPM packages.

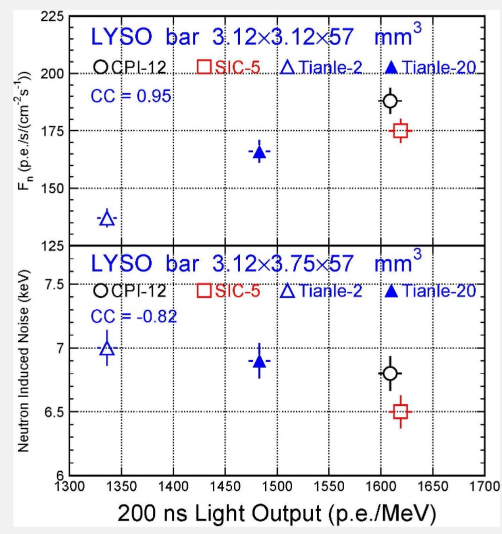

Fig. 12 Correlation between Fn (top) and RIN:n (bottom) vs. the LO in 200 ns for four LYSO+SiPM packages.

Fig. 7 shows the setup for the RIN:γ and RIN:n experiments. Fig. 8 shows the layout of the neutron source assembly consisting of three cylindrical Cf-252 source pairs. Fig. 9 shows histories of photocurrent measured for CPI-12 (top) and SIC-5 (bottom) LYSO+SiPM packages under Co-60 irradiation of 120, 185 and 250 rad/h. Fig. 10 shows the photocurrent measured during irradiation as a function of the dose rate with a good linearity. Figs. 11 and 12 show an excellent correlation between the F_γ and F_n (top) and RIN:γ and RIN:n (bottom) vs. the LO in 200 ns gate, and the RIN:γ and RIN:n values of about 34 and 7 keV respectively, much less than the 4.2 MeV signal expected from minimum ionization particles.

3. Ultrafast Yttrium Doped BaF_2 Crystals

3.1 Ultrafast and Radiation Hard BaF_2 Crystals

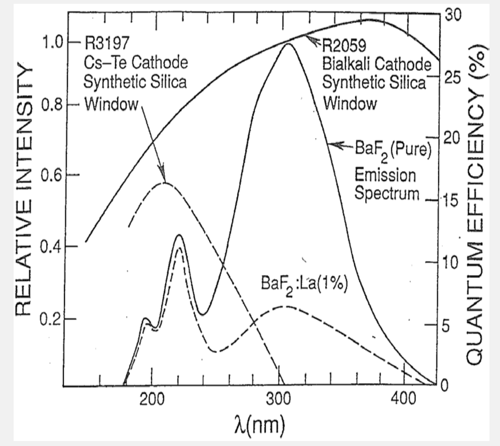

Fig. 13 BaF_2 emission and QE of various vacuum PMTs.

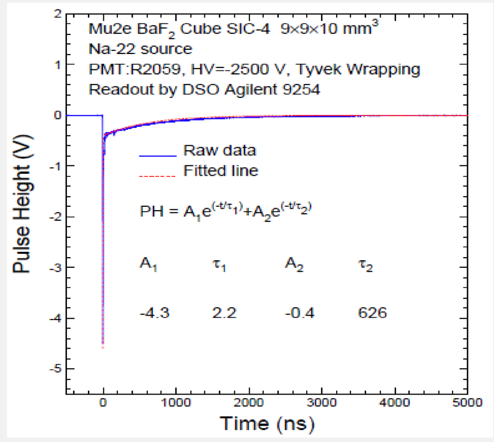

Fig. 14 Pulse shape of BaF_2 crystal measured by a PMT.

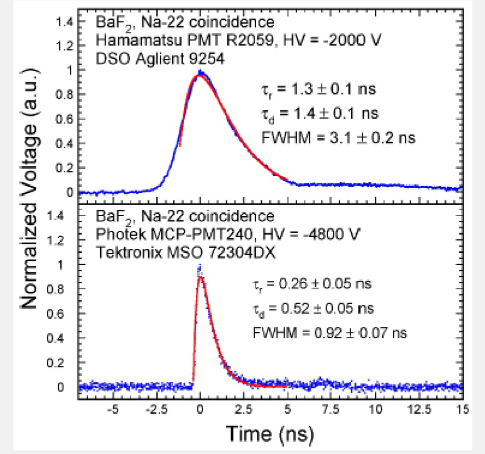

Fig. 15 Pulse shape of BaF_2 crystal measured by a PMT and a MCP-PMT.

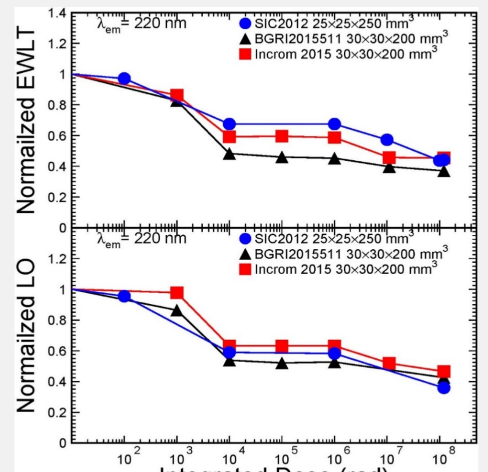

Fig. 16 Normalized EWLT and LO of 20 cm BaF_2 crystals up to 130 Mrad.

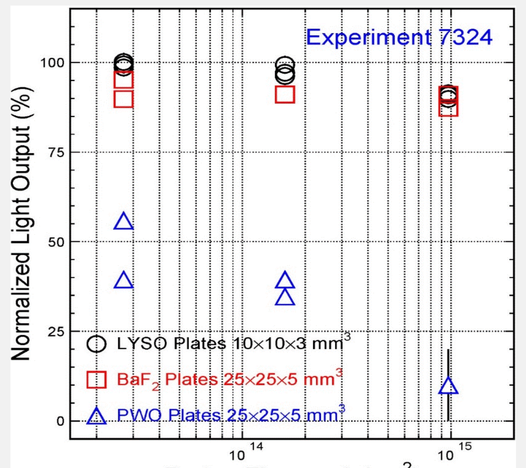

Fig. 17 Normalized LO of BaF_2 crystals after protons up to 9.7×10^{14} p/cm².

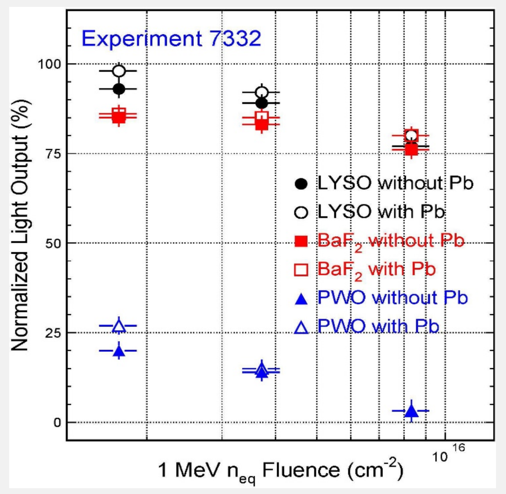

Fig. 18 Normalized LO of BaF_2 after neutrons up to 8.3×10^{15} n_{eq}/cm^2.

Figs. 13 shows BaF_2 emission and QE of PMTs with bialkali and solar-blind cathode. The ultrafast light @ 220 nm with **0.5 ns** decay time requires a VUV-sensitive photodetector, and the slow light @ 300 nm which may be suppressed by either La doping in BaF_2 or a solar-blind PMT. Figs 14 and 15 show BaF_2 pulse shape measured by a PMT and a much-faster MCP-PMT. Fig. 16 shows γ-ray induced damage in 20 cm long BaF_2 crystals saturates from 10 krad to 130 Mrad. Figs. 17 and 18 confirm the saturation damage in BaF_2 from protons and neutrons respectively. It is clear that BaF_2 plates of a few mm thick survive proton and neutron irradiation up to 9.7×10^{14} p/cm² and 8.3×10^{15} n_{eq}/cm^2, respectively.

3.2 Slow Suppression by Yttrium Doping in BaF_2

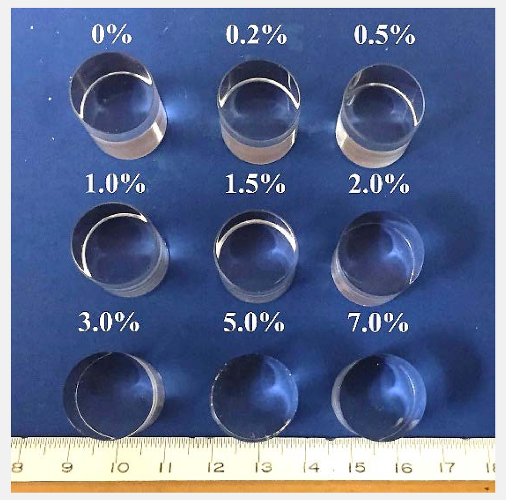

Fig. 19 Nine BaF_2 crystal cylinders of $\Phi18\times21$ mm³ grown at BGRI with various Y-doping levels.

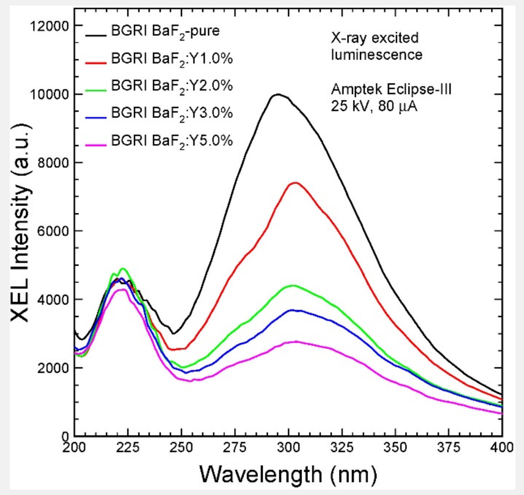

Fig. 20 XEL spectra for five BaF_2 cylinders with various yttrium-doping levels.

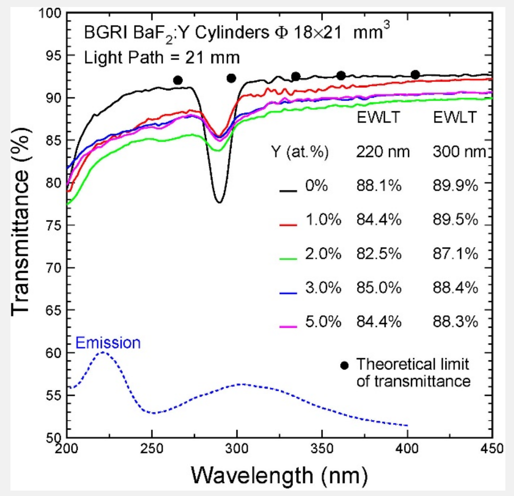

Fig. 21 Transmittance and XEL spectra for five BaF_2 cylinders with various yttrium-doping levels.

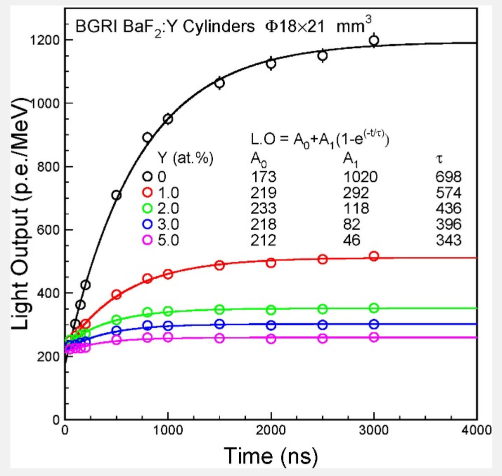

Fig. 22 LO as a function of the integration time for BaF_2 cylinders with different yttrium-doping levels

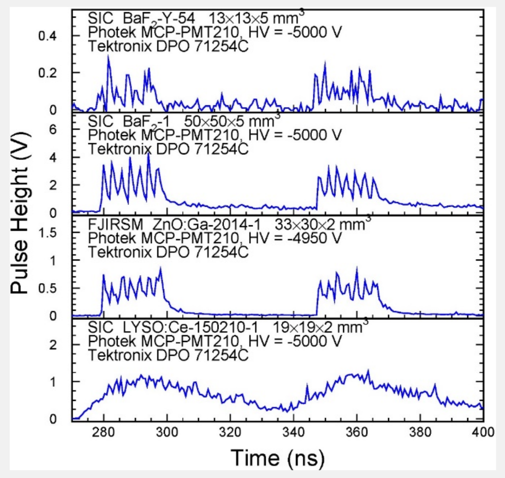

Fig. 23 Imaging for 2 septuplet bunches measured by BaF_2:Y, BaF_2, ZnO:Ga, and LYSO:Ce, respectively

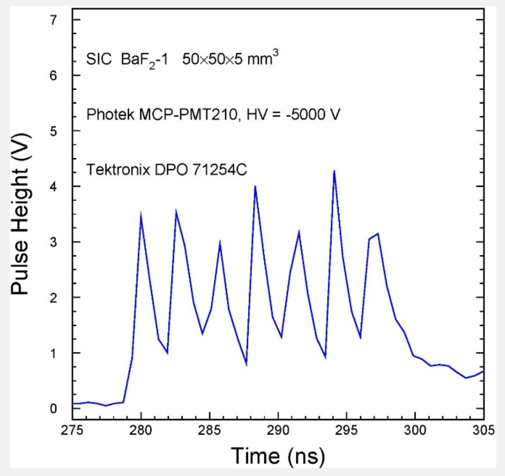

Fig. 24 BaF_2 imaging for 2.83 ns bunch spacing

Fig. 19 shows nine BaF_2 cylinders of $\Phi18\times21$ mm³ grown at BGRI with different Y^{3+} doping levels. Fig. 20 shows the XEL peaks at 220 and 300 nm for the fats and slow light, showing a reduced slow light intensity for increased yttrium doping level, while the intensity of the fast emission is consistent. Fig. 21 shows the transmittance spectra (solid lines) measured along 21 mm light path for all samples. Fig. 22 shows LO as a function of integration time for these samples, confirming a reduced slow component and consistent fast component. Figs. 23 and 24 shows the response of BaF_2 and BaF_2:Y to septuplet X-ray bunch with 2.83 ns bunch spacing, providing a proof of principle for the ultrafast inorganic scintillator-based front imager for GHz hard X-ray imaging.

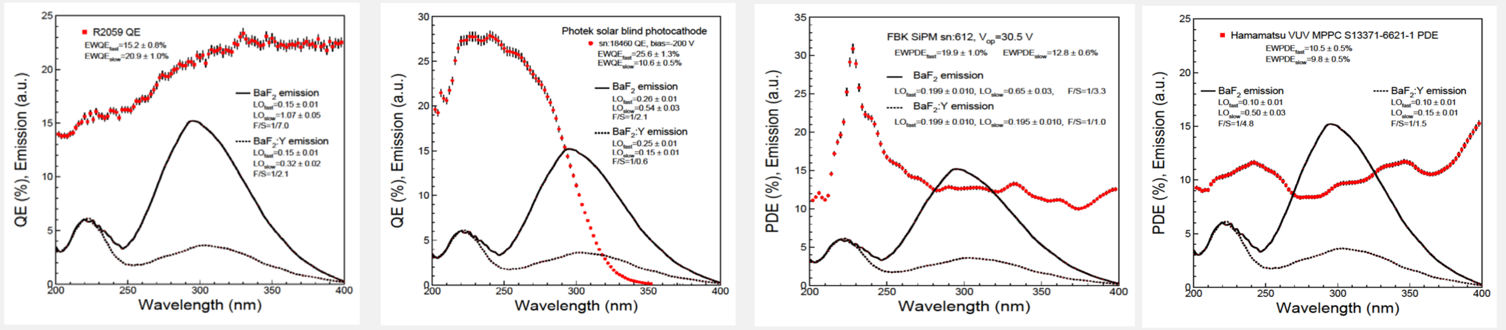

Fig. 25 The measured QE (200-400 nm) of four VUV photodetectors (from left to right): Hamamatsu R2059 PMT, Photek solar blind photocathode, FBK SiPM integrated with type-I UV filter, and Hamamatsu VUV MPPC.

Fig. 25 shows the measured QE of four VUV photodetectors. While yttrium doping in BaF_2 crystals increases its F/S ratio significantly a solar-blind photodetector is also needed to minimize the pileup for a BaF2 crystal based ultrafast calorimeter for future experiments, such as Mu2e-II.

4. Summary

- Bright, fast and radiation hard inorganic scintillators are needed for future HEP experiments at the HL-LHC and FCC-hh. Our data show that mm thick plates of LYSO:Ce crystal and LuAG:Ce ceramics survive 10^{15} p/cm² and 10^{16} n_{eq}/cm^2, so are promising materials in severe radiation environment.
- The RIN:γ and RIN:n experiments carried out for four LYSO+SiPM packages show the RIN:γ and RIN:n values of about 34 keV under 200 rad/h and 7 keV under the neutron flux of 3.2×10^6 $n_{eq}/cm^2/s$, which are negligible as compared to the 4.2 MeV MIP signal for the CMS BTL detector. The result also indicates that the radiation induced readout noise *in situ* is dominated by ionization dose.
- Undoped BaF_2 crystals provide ultrafast light with sub-ns decay time and a good radiation hardness up to 130 Mrad. Yttrium doping suppresses its slow light and promises an ultrafast inorganic scintillator with much reduced slow contamination. R&D is going for developing both yttrium doped BaF_2 and solar-blind VUV photo-detectors for future HEP experiments, such as Mu2e-II.

Acknowledgments: This work is supported by the U.S. Department of Energy, Office of High Energy Physics program under Award Number DE-SC0011925.

Contact : zhu@hep.caltech.edu